

# Development and Evaluation of an Identification Method for the Biomechanical Parameters Using Robotic Force Measurements, Medical Images, and FEA

Takeharu Hoshi, Mariko Tsukune, Yo Kobayashi, Tomoyuki Miyashita, and Masakatsu G. Fujie

**Abstract**— This paper presents a new identification method for the biomechanical parameters of human tissues for the purpose of improving the accuracy of dynamic organ simulation. We describe the formulation of the method, and also design a robotic system to implement the method using a robotic probe, a medical imaging device, and a numerical simulator for the finite element analysis (FEA). We carried out an experiment using an experimental system and a tissue phantom to verify the effectiveness of the method. The results of this experiment show that the Young's modulus of the tissue phantom can be estimated with the experimental system. We also compared the estimated values of the Young's moduli with the measured values from a rheometer. These results confirm that the identification method and the system design, proposed and developed in this work, are effective for accurately simulating organ behavior.

## I. INTRODUCTION

ONE of the most challenging issues in the area of robot assisted surgery (RAS) is the development of control methods for surgical robots to manipulate soft tissue in the human body. Key examples of such soft regions include the breast, liver, and brain, with tumor of each of these recognized as a disease with global public health implications. Here, there is a peculiar difficulty derived from the characteristics of soft tissue; that is, organ deformation. The manipulation site is very soft, and it is easy for the force of the surgical tool to deform the tissue and, as a result, for the position of the target tumor to be displaced. Thus, surgical robots require control methods that compensate for tissue deformation to achieve a high level of accuracy.

Several research groups have proposed surgical robot control methods to account for the soft tissue deformation by using deformable organ models. The robot control methods, which we call “organ model-based control methods,”

Manuscript received April 15, 2011. This work was supported in part by the Global COE Program “Global Robot Academia” from MEXT (Ministry of Education, Culture, Sports, Science and Technology of Japan), High-Tech Research Center Project from MEXT, Grant-in-Aid for Scientific Research from MEXT (no. 22360108, no. 22103512), and Waseda University Grant for Special Research Projects (no. 2010B-177).

T. Hoshi is with the Faculty of Science and Engineering, Waseda University, Shinjuku-ku, 3-4-1 Okubo, Tokyo, Japan (corresponding author: phone: +81-3-5286-3412; Fax: +81-3-5291-8269; E-mail: hoshi@aoni.waseda.jp).

M. Tsukune is with the Graduate School of Science and Engineering, Waseda University, Tokyo, Japan.

Y. Kobayashi, T. Miyashita, and M. G. Fujie are with the Faculty of Science and Engineering, Waseda University, Tokyo, Japan.

consider organ deformation using model-based numerical analyses so that precise and safe treatment can be realized. For example, Okamura *et al.* developed models for needle insertion force, tissue stiffness, friction force, and puncture force [1]. DiMaio and Salcudean proposed a system to measure the extent of planar tissue phantom deformation during needle insertion [2], [3]. Alterovitz, Goldberg and Okamura investigated the simulation of steerable needle insertion for prostate therapy [4], [5]. The authors reported the material properties of the liver to realize physically accurate deformable models, and investigated physical organ modeling for use in a surgical robot control method [6]-[8]. The authors also developed an integrated system with image guidance and deformation simulation for the purpose of accurate needle insertion [9].

Although organ model-based control methods have been expected to solve the problem of compensating tissue deformation as previously mentioned, an additional identification method for biomechanical properties of tissues in the target region is necessary to provide a reliable and practical RAS system. The performance of an organ model-based control method depends on the accuracy of the model behavior, which demands that material parameters be precisely defined. At the same time, however, it is difficult to determine the biomechanical properties of human tissues for the following two reasons. First, there is no method by which to measure accurately, directly, and non-invasively the distribution of tissue properties in the human body. Second, individual differences in the properties of human tissues, which inherently vary as a result of factors such as age, sex, clinical history, and living habits, make it increasingly difficult to determine the values of the material parameters. Thus, if no method for quantifying material parameters of human tissues is developed, the use of computer assisted dynamic simulation may lead to a reliability problem from a medical point of view.

We have focused on the problem of uncertainty in the biomechanical parameters of human organ models, and in this work we propose a new method that allows the biomechanical parameters of human tissues to be identified. The primary objective of this paper is to present a new method to identify the values of the biomechanical parameters of human tissues. More specifically, this paper gives the formulations and a system design for the method. The secondary objective is to demonstrate the efficacy as well as the limitations of the proposed method based on experiments with a tissue phantom

and an experimental system, which uses force sensing data, ultrasound images, and finite element analysis (FEA). These efforts contribute to creating guidelines for developing new medical systems to identify the biomechanical parameters of human tissues.

The rest of this paper is organized as follows. Section II presents the related works for this study, while Section III introduces the proposed method. Section IV discusses the experimental conditions to verify the proposed method. In Section V we present the experimental results and a validation thereof. We also discuss the efficacy and limitations of the method based on the results. Finally, Section VI presents our conclusions and describes areas for future research.

## II. RELATED WORKS

In this section, we briefly review research related to biomechanical parameter identification problems. We have grouped the related works into the following two areas.

1) *Elasticity imaging*: An approach is a measurement technique generally known as elastography, which involves the use of static or oscillatory deformations and sequential images during deformation using medical modalities such as MRI or ultrasound equipment [10]-[12]. These techniques are useful for enabling medical staff to real-time visualize the distribution of tissues in the human body. The ability thereof to quantify biomechanical properties, however, is limited because the techniques typically depend on relative displacements field between sequential images.

2) *Inverse analysis*: The other category is inverse analysis using a dynamic model of behavior of the tissue. The major advantages of this approach are accuracy and compatibility with simulations using models such as the finite element model (FEM). Hence, in recent years, several research projects have investigated identification methods for biological tissue properties. Wang *et al.* [13], [14] researched an identification method for properties of rheological objects based on a FE formulation. Sangpradit *et al.* [15] introduced the concept of a robotic indentation tool using FEA, and showed preliminary experiments for it. We researched the problem of determining the values of human material parameters for surgical use [16], [17]. In a previous work [17], we proposed a robotic palpation system to identify the biomechanical properties, and also pointed out potential limitations of systems dependently based on contact force measurements like palpation. Miga *et al.* addressed the inverse analysis method by using the FEM and medical images through which to identify the values of the model parameters [18], [19]. These works revealed the potential of the simultaneous use of measurement force and medical imaging to determine the properties of tissues. However, practical implementations of this kind of system and the validation thereof have not yet been reported in any detail, even though the conventional works have proposed conceptual schemes and basic numerical tests. In this paper, we report phantom experiments to evaluate a system to

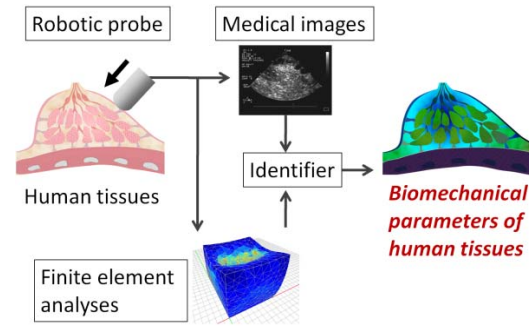


Fig. 1. The conceptual scheme of our proposed method for providing spatially distributed values of the biomechanical parameters of human tissue.

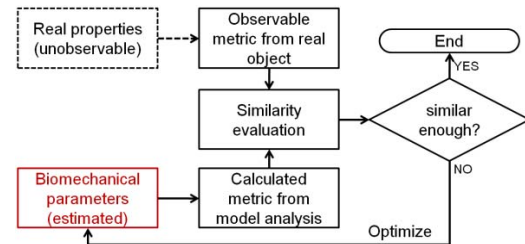


Fig. 2. The basic idea of our proposed method for identifying biomechanical parameters based on inverse analysis.

identify the biomechanical properties of tissues, where the system integrates robotics, medical imaging, and FEA components. It should be noted that the present paper contributes to the detailed presentation of our method, as well as to the validation thereof through a phantom experiment.

## III. METHOD

The basic concept of the proposed method for identification of the biomechanical parameters of human tissues is to compare the behavior of the simulated tissue deformations obtained by model analyses with the actual deformations obtained by a robotic sensing system. We see this strategy as being a kind of inverse analysis problem. The reason for this is that the distribution of the biomechanical parameters, which determines the behavior of the human body deformation, must be estimated from the available measurements, which are related to the tissue deformation (Fig. 1, Fig. 2). In consideration of this scheme, we need to define metrics for similarity by which to evaluate the reproducible degree of the estimated values of the parameters. Here, medical images are useful as metrics for two reasons. First, medical images (e.g., ultrasound images) have the ability to show the deformation of the internal body, which is related to the factors of biomechanical properties in the human body. Second, there are several algorithms to measure similarity between two different images [20].

Based on the above considerations, we propose a new robotic method, the framework of which incorporates various components (Fig. 3), and its formula to identify the biomechanical parameters using medical images. The

biomechanical parameters are identified so as to minimize the cost function, which is evaluated in a similarity evaluation using the medical images. The components of the proposed system are as follows.

1) *Sensing manipulator*: The robotic manipulator is considered a data acquisition tool. The proposed system incorporates sensors for measuring the contact force and displacement at the point of contact on the human body by the robotic probe as well as devices for imaging the deformation of the internal body.

2) *Finite element analysis*: We used the finite element method for tissue deformation modeling. In this paper, we consider only the linear static cases to simplify the problem and to keep the paper to a reasonable length. In this case, the relation between displacement and force is described by the FEM as the following linear algebraic equation:

$$\mathbf{f} = \mathbf{K}\mathbf{u} \quad (1)$$

where  $\mathbf{f}$ ,  $\mathbf{K}$ , and  $\mathbf{u}$  are the force vector, stiffness matrix, and displacement vector, respectively. In the finite element theory, the biomechanical properties  $\theta$  for each element area are associated with the stiffness matrix  $\mathbf{K}$  [17]. Therefore, inverse analysis of the biomechanical parameters through FEA is available using measured values of force and displacement.

3) *Image warping using FEA*: In the proposed method, a procedure of image warping through FEA is used to generate the metrics to measure the reproducibility of the real deformation of an object. The warped image is generated to be a simulation of an object in the deformation state from an image, which we call the “source image”, in the pre-deformation state. Image warping is carried out using the deformation field between pre- and post-displacement, which is calculated by FEA (Fig. 4). Here, since the displacement data at each nodal point in the FEA are spatially discretized, in this paper thin-plate spline (TPS) interpolation, which has been widely used as a non-rigid transformation method [20], [21], is carried out to generate a continuous deformation field.

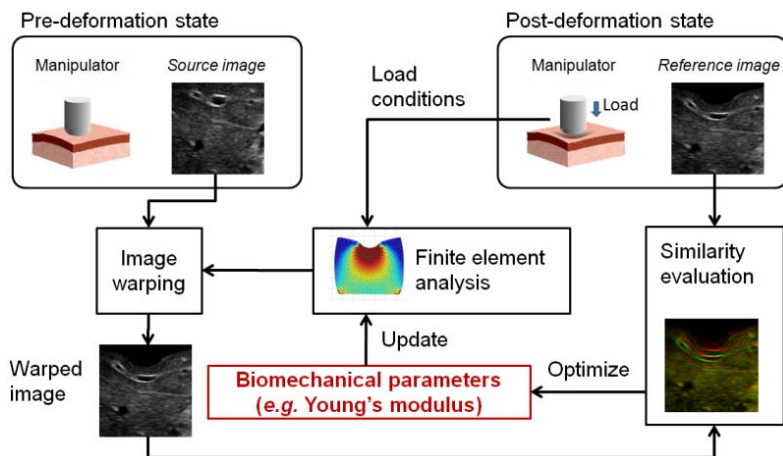


Fig. 3. Overview of the proposed method. The framework incorporates a robotic force measurement component, a medical imaging component, and a finite element analysis component. The biomechanical parameters are identified to minimize the cost function, which is evaluated by the similarity evaluation process.

4) *Similarity evaluation*: In this paper, normalized mutual information (NMI) [20] is used as a similarity measure between the warped image and the image in the post-deformation state, which we call the “reference image”. NMI evaluates the similarity of two images using information-theoretic measures. Since a considerable number of studies have, in recent years, reported on the superior features of NMI for medical use, we chose this as the similarity metric for the proposed method. Here, the cost function to evaluate is described using NMI as

$$Cost(\theta) = - Similarity_{NMI} ( Image^{warped}(\theta), Image^{reference} ). \quad (2)$$

We assume that the warped images will be most similar at the time when appropriate values of model parameters are set. Figure 5 shows the tendency of the relationship between the similarity measure and the subtraction of images.

5) *Parameter identification*: Given the above, the proposed framework shown in Fig. 3 is available to identify the biomechanical parameters  $\theta$  in the FE-model to minimize the difference between the warped image from the source and the reference image.

$$\theta^* = \underset{\theta}{\operatorname{argmin}} (Cost(\theta)) \quad (3)$$

The values of the parameters can be improved even during execution of the framework.

#### IV. EXPERIMENTAL CONDITIONS

In this section, we describe the conditions under which we conducted the experiment. The proposed method was executed using the test system we implemented. Given below are the details of our experimental setup.

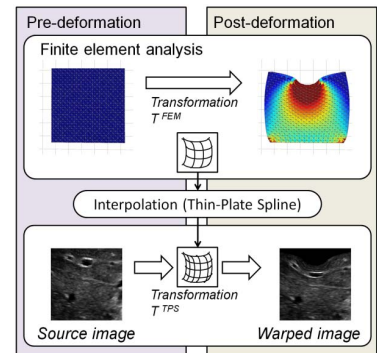


Fig. 4. Image warping using the deformation field generated by FEA. The continuous deformation field is calculated from the discretized deformation field in each nodal point on the FE-mesh.

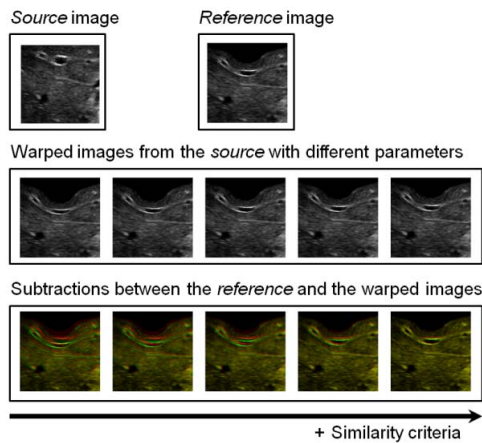


Fig. 5. Relationship between the similarity criteria and the subtraction of two different images. A warped *source* image and the *reference* image are displayed in red and green layers, respectively, in the same subtraction image.

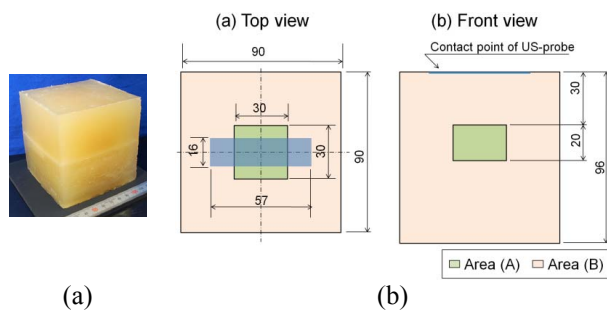


Fig. 6. The phantom in the experiment. (a) Overview. (b) The size of the phantom.

TABLE I  
WEIGHT RATIO PERCENTAGES OF THE PHANTOM AREAS A/B

	Area (A)	Area (B)
Water	68.0	69.3
Gelatin	29.1	14.9
Sucrose	0.0	14.2
Cellulose	2.9	1.0
Citric acid	0.0	0.4
Pectin	0.0	0.2

### A. Phantom

Tissue-mimicking gelatin phantom was used as the organ phantom in the experiment. The materials were designed to provide the similar mechanical and ultrasonic characteristics of the biological tissue [22], [23]. Areas of (A) and (B) in the phantom simulated the tumor and the surrounding normal tissue (Fig. 6). The phantom was made into a rectangular solid (length: 90 mm, width: 90 mm, height: 96 mm). The mixture weight percentages of the areas were shown in Table 1. We measured the actual stiffness of the areas in the phantom. Figure 7 shows the relation between shear stress and strain as measured by a rheometer (AR-G2, TA-Instrument, USA). Since gelatin is sensitive to temperature, the sample and the phantom were cooled to keep 5 °C during the measurement and the experiment. Using linear regression analysis, we determined that the shear modulus of the area (A) and the area (B) were approximately  $G_A = 21$  kPa and  $G_B = 6.0$  kPa, respectively, where they were

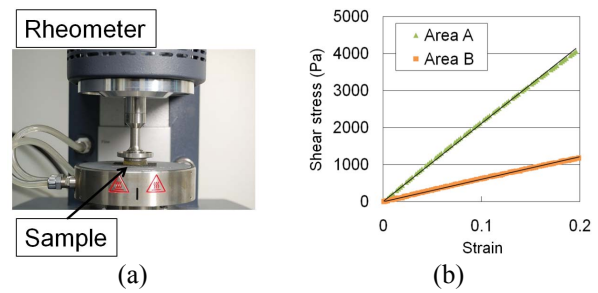


Fig. 7. Elasticity properties of the gelatin phantom. (a) Rheometer (b) Relation of shear stress and strain

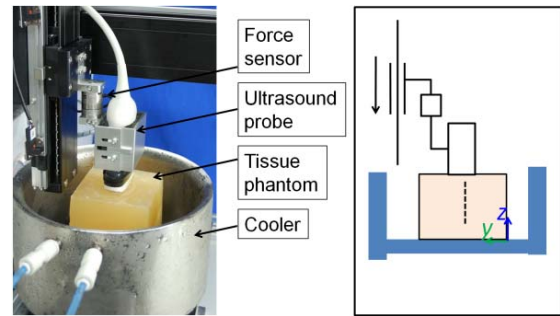


Fig. 8. The experimental setup.

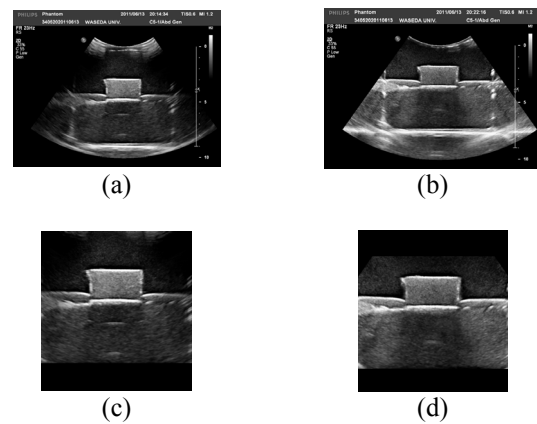


Fig. 9. The ultrasound images. (a) Original image for the pre-deformation. (b) Original image for the post-deformation. (c) ROI of the pre-deformation (*source* image). (d) ROI of the post-deformation (*reference* image).

regarded as linear elastic objects. The relation between the Young's modulus  $E$  and the shear modulus  $G$  of a linear elastic object is calculated using Poisson's ratio  $\nu$  as follows:

$$E = 2(1 + \nu) G. \quad (4)$$

It appears that Poisson's ratio for biological objects generally has a value close to 0.5. Thus, the approximate values of the Young's modulus for the areas were approximated as  $E_A = 63$  kPa and  $E_B = 18$  kPa, respectively.

### B. Experimental manipulator

An experimental manipulator, with one degree of freedom of linear movement by an actuator, was used to measure the load condition. A force sensor (MICRO 5/50-SA, BL AUTOTEC Ltd., Japan) and an ultrasound probe were



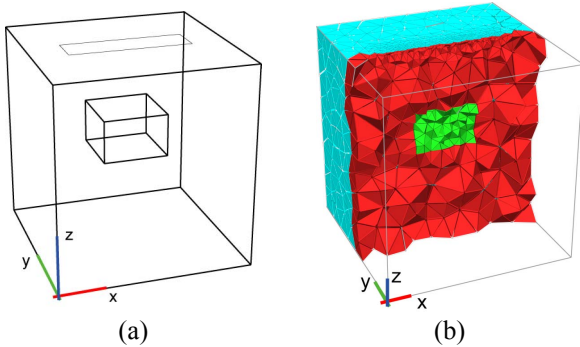


Fig. 10. The FEA conditions. (a) Regional condition. (b) Mesh data.

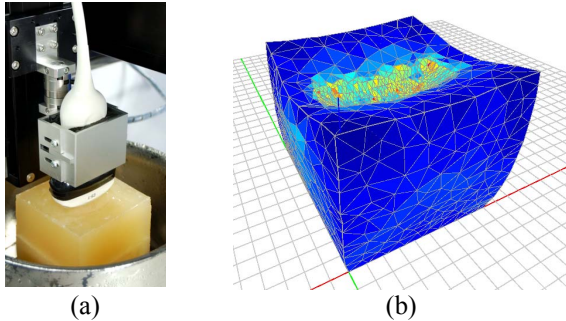


Fig. 11. The post-deformation state in the experiment. (a) Phantom. (b) FEA.

attached to the manipulator (Fig. 8). The reactive forces exerted on the probe were sampled by the force sensor. We calculated the moving distance of the probe from the value of the encoder attached to the motor.

In the experiment, two datasets of ultrasound images and the measured reactive force were obtained. The first dataset includes an image for the *source* at the time when the reactive force is approximately zero. The other dataset includes an image for the *reference* at the time when the force is 9.0 N and the moving distance is 14.8 mm. Figure 9 shows the images and their region of interest (ROI) to evaluate the similarity. Ultrasound equipment (iU22, Philips) was used as the imaging modality in the experiment. This equipment is compatible with the proposed method due to the compactness of the probe and its ability for real-time visualization.

### C. Finite element analysis and image warping

A FEM simulator was used to analyze the deformation during the load. In the experiment, we used a three-dimensional linear elastic model. The FE model used in the experiment includes 2853 nodes and 14029 elements. A conforming Delaunay tetrahedralization (CDT) was performed to generate the mesh data for the FEA, by using a well-regarded mesh generator TetGen [24] (Fig. 10). In this experiment, the software for FEA (Fig. 11), TPS, and NMI were implemented in C++ and Python by the authors.

### D. Biomechanical parameters and identification

For these experiments, we chose the Young's modulus as the material property to be analyzed as this is one of the most important material parameters of the biological tissues in the deformation problem. In this experiment, we assumed

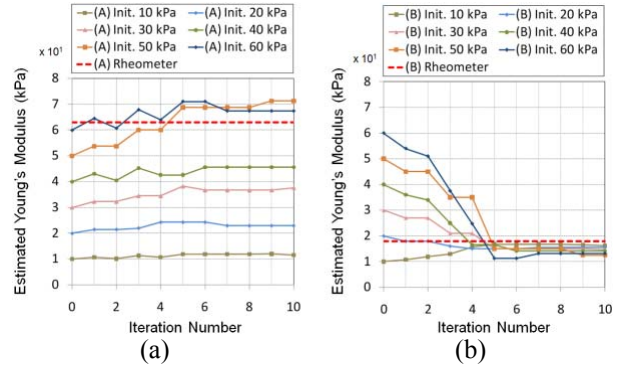


Fig. 12. Estimation process of the Young's modulus of each area. (a) and (b) shows the results in the areas of (A) and (B), respectively. The initially estimated Young's modulus are 10 kPa, 20 kPa, 30 kPa, 40 kPa, 50 kPa, and 60 kPa. The Young's modulus measured by the rheometer was shown as the dashed line.

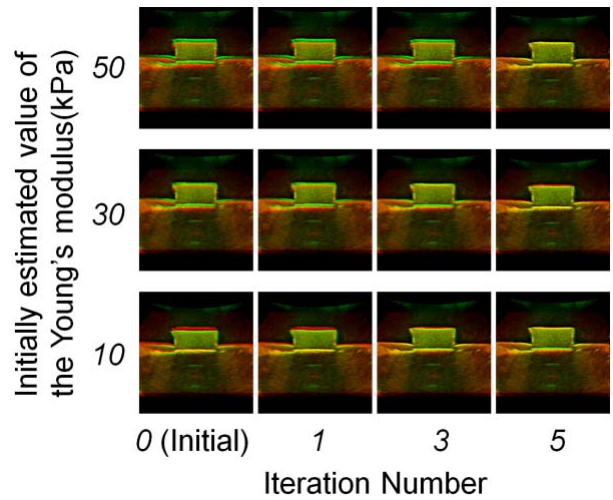


Fig. 13. The subtraction images in the estimation process. A warped *source* image and the *target* image are displayed in red and green layers, respectively, in the same subtraction image. The initially estimated Young's modulus are 10 kPa, 30 kPa, and 50 kPa, respectively. The similarity of the image improved with the iterative optimization by the method.

uniformity of the phantom tissue. In this paper, the identification process was carried out using the downhill simplex method to minimize the cost function and concurrently optimize the values in the parameter vector  $\theta$  of the FE model, for which the method is a fast, general-purpose optimization approach to solving nonlinear problems. Under the consideration, the biomechanical parameters  $\theta$  to be identified can be written as  $\theta = \{E_A, E_B\}$ .

## V. RESULTS AND DISCUSSION

In this section, we present the experimental identification results using the proposed system. We also discuss the efficacy and the limitations of the method based on the results.

Estimation experiments of the Young's modulus were carried out using our test system. In the experiment, we assumed various values to be the initial estimation values of the Young's moduli as shown in Fig. 12. In the experiment,

the experimental setup we implemented worked well as we had designed. The values of the estimated Young's modulus in the area (A) and (B) in the phantom were concurrently optimized by the experimental system. The estimated Young's modulus of the area (B) converged to the appropriate order compared with the measured values by rheometer. Therefore, this robot-assisted identification is a promising method. On the other hand, however, the Young's modulus of the area (A) was not sensitively estimated by the method. The findings from the present investigation suggest further studies of possible factors, including analyses of the stability, sensitivity, and accuracy of the identification algorithm, the effects of the volume occupied by the tissues, etc.

## VI. CONCLUSION

The purpose of our research was to develop a method to identify the values of the biomechanical parameters of human tissues. In this paper, we presented a new method and the design of a system to provide the parameters. The proposed system incorporates a robotic force sensing system, medical imaging system, and a numerical dynamic simulation system using FEA. We also described the method and the formulation of the proposed system. In experiments using a test system and a tissue phantom were carried out to demonstrate the feasibility of the proposed method. The experimental results reveal that the proposed method has the ability to quantitatively determine the elastic modulus of tissues. Several potential challenges regarding the future of this system are also discussed.

We intend performing further analyses based on the findings obtained in this study. In addition, we will analyze studies on the complexities of properties of human tissues since these have mostly been conducted under the assumption that the tissues have inhomogeneous, anisotropic elastic and viscous, and non-linear behaviors, as recently reported [25]. We also intend developing a more practical system for clinical use that integrates the robotic system and dynamic simulation system.

## REFERENCES

- [1] A. M. Okamura, C. Simone, and M. D. O'Leary, "Force modeling for needle insertion into soft tissue," *IEEE Trans. Bio-med. Eng.*, vol. 51, no. 10, pp. 1707-1716, Oct. 2004.
- [2] S. P. DiMaio and S. E. Salcudean, "Needle insertion modeling and simulation," *IEEE Trans. Robot. Autom.*, vol. 19, no. 5, pp. 864-875, Oct. 2003.
- [3] S. P. DiMaio and S. E. Salcudean, "Needle steering and motion planning in soft tissues," *IEEE Trans. Bio-med. Eng.*, vol. 52, no. 6, pp. 965-974, June 2005.
- [4] R. Alterovitz, K. Goldberg, and A. Okamura, "Planning for steerable bevel-tip needle insertion through 2D soft tissue with obstacles," in *Proc. 2005 IEEE Int. Conf. Robotics and Automation (ICRA 2005)*, pp. 1640-1645.
- [5] R. Alterovitz, A. Lim, K. Goldberg, G. S. Chirikjian, and A. M. Okamura, "Steering flexible needles under Markov motion uncertainty," in *Proc. 2005 IEEE/RSJ Int. Conf. Intelligent Robots and Systems (IROS'05)*, pp. 1570-1575.
- [6] Y. Kobayashi, A. Kato, T. Hoshi, K. Kawamura, and M. G. Fujie, "Parameter setting method considering variation of organ stiffness for the control method to prevent overload at fragile tissue," in *Proc. 2009*

- IEEE Int. Conf. Intelligent Robots and Systems (IROS'09)*, pp. 2155-2161.
- [7] Y. Kobayashi, A. Onishi, H. Watanabe, T. Hoshi, K. Kawamura, and M. G. Fujie, "Developing a planning method for straight needle insertion using probability-based condition where a puncture occurs," in *Proc. 2009 IEEE Int. Conf. Robotics and Automation (ICRA'09)*, pp. 3482-3489.
- [8] Y. Kobayashi, A. Onishi, T. Hoshi, K. Kawamura, M. Hashizume, and M. G. Fujie, "Development and validation of a viscoelastic and nonlinear liver model for needle insertion," *Int. J. Comp. Assisted Radiol. and Surgery (CARS)*, vol. 4, no. 1, pp. 53-63, 2009.
- [9] Y. Kobayashi, A. Onishi, H. Watanabe, T. Hoshi, K. Kawamura, M. Hashizume, and M. G. Fujie, "Development of an integrated needle insertion system with image guidance and deformation simulation," *Int. J. Computerized Med. Imaging and Graphics (CMIG)*, vol. 34, no. 1, pp. 9-18, 2010.
- [10] J. Ophir, S. K. Alam, B. Garra, F. Kallel, E. Konofagou, T. Krouskop, and T. Varghese, "Elastography: ultrasound estimation and imaging of the elastic properties of tissues," in *Proc. Inst. Mech. Eng. Part H: J. Engineering in Medicine*, vol. 213, no. 3, pp. 203-233, 1999.
- [11] M. Fatemi, L. E. Wold, A. Alizad, and J. F. Greenleaf, "Vibro-acoustic tissue mammography," *IEEE Trans. Med. Imaging*, vol. 21, no. 1, pp. 1-8, Jan. 2002.
- [12] B. J. Fahey, K. R. Nightingale, S. A. McAleavey, M. L. Palmeri, P. D. Wolf, G. E. Trahey, "Acoustic radiation force impulse imaging of myocardial radiofrequency ablation: initial in vivo results," *IEEE Trans. Ultrasonics, Ferroelectrics and Frequency Control*, vol. 52, no. 4, pp. 631-641, April 2005.
- [13] Z. Wang, K. Namima, and S. Hirai, "Physical parameter identification of rheological object based on measurement of deformation and force," in *Proc. 2009 IEEE Int. Conf. Robotics and Automation*, pp. 1238-1243.
- [14] Z. Wang and S. Hirai, "Modeling and property estimation of Japanese sweets for their manufacturing simulation," in *Proc. 2010 IEEE/RSJ Int. Conf. Intelligent Robots and Systems (IROS 2010)*, Taipei, pp. 3536-3541.
- [15] K. Sangpradit, H. Liu, L. D. Seneviratne, and K. Althoefer, "Tissue identification using inverse finite element analysis of rolling indentation," in *Proc. 2009 IEEE Int. Conf. Robotics and Automation*, pp. 1250-1255.
- [16] T. Hoshi, Y. Kobayashi and M. G. Fujie, "Developing a system to identify the material parameters of an organ model for surgical robot control," in *Proc. 2008 IEEE Biomedical Robotics and Biomechatronics (BioRob'08)*, pp. 730-735.
- [17] T. Hoshi, Y. Kobayashi, T. Miyashita, and M. G. Fujie, "Quantitative palpation to identify the material parameters of tissues using reactive force measurement and finite element simulation," in *Proc. 2010 IEEE Int. Conf. Intelligent Robots and Systems (IROS'10)*, pp. 2822-2828.
- [18] C. W. Washington and M. I. Miga, "Modality independent elastography (MIE): a new approach to elasticity imaging," *IEEE Trans. Med. Imaging*, vol. 23, no. 9, pp. 1117-1128, Sept. 2004.
- [19] J. J. Ou, R. E. Ong, T. E. Yankeelov, and M. I. Miga, "Evaluation of 3D modality-independent elastography for breast imaging: a simulation study," *Phys. Med. Biol.*, 53, pp. 147-163, 2008.
- [20] W. R. Crum, T. Hartkens, and D. L. G. Hill, "Non-rigid image registration: theory and practice," *British J. Radiol.*, vol. 77, pp. S140-S153, 2004.
- [21] T. M. Lehmann, C. Gonner, and K. Spitzer, "Survey: interpolation methods in medical image processing," *IEEE Trans. Med. Imaging*, vol. 18, no. 11, pp. 1049-1075, Nov. 1999.
- [22] Ernest L Madsen et al, "Tissue-mimicking agar/gelatin materials for use in heterogeneous elastography phantoms," *Physics in Medicine and Biology*, vol. 20, pp. 5597-5618, 2005
- [23] Pavan, T.Z.; Carneiro, A.A.O.; Madsen, E.L.; Frank, G.R.; Hall, T.J.; , "Exploring the nonlinear elastic behavior of phantoms materials for elastography," *Ultrasonics Symposium (IUS)*, 2009 IEEE International , vol., no., pp.463-466, 20-23 Sept. 2009
- [24] Hang Si, "TetGen: A Quality Tetrahedral Mesh Generator and a 3D Delaunay Triangulator", <http://tetgen.berlios.de/>
- [25] M. Tsukune, Y. Kobayashi, T. Hoshi, T. Miyashita, and M. G. Fujie, "Evaluation and comparison of the nonlinear elastic properties of the soft tissues of the breast," in *Proc. 2011 Int. Conf. IEEE Engineering in Medicine and Biology Society (EMBC'11)*, (Accepted).